Soft Matter

Accepted Manuscript

ROYAL SOCIETY OF CHEMISTRY

www.rsc.org/softmatter

The solvent dynamics at pore surfaces in molecular gels studied by field-cycling magnetic resonance relaxometry

Jadwiga Tritt-Goc*, Adam Rachocki and Michał Bielejewski

Institute of Molecular Physics, Polish Academy of Sciences, M. Smoluchowskiego 17, 60-179 Poznań, Poland

*Address for correspondence:

Prof. Dr. Hab. Jadwiga Tritt-Goc
Institute of Molecular Physics, PAS
M. Smoluchowskiego 17
60-179 Poznań, Poland
phone: +48-061 8695-226
e-mail: jtg@ifmpan.poznan.pl

Abstract

The molecular dynamics of the solvent molecules at liquid-solid interfaces in low molecular mass gels and in bulk solvents have been identified and characterized with the aid of field-cycling NMR relaxometry. The gels are formed by ethylene glycol (EG) and 1,3-propanediol (PG) with different concentrations of 4,6,4',6'-O-Terephthylidene-bis(methyl α-D-glucopyranoside) (gelator **1**). The spin-lattice relaxation times of bulk solvents measured in the function of Larmor frequency were analyzed assuming the intramolecular and intermolecular dipole-dipole interactions. For analysis of the relaxation data for confined solvents the two-phase fast-exchange model was assumed. It was found that in a low-frequency range a dominating NMR relaxation mechanism of solvent interacting with internal surfaces of pores in studied molecular gels is reorientations mediated by translational displacements (RMTD). This dynamic process allows us to explain a very long correlation time of the order of 10^{-5} s calculated for confined EG molecules and even longer one for PG. The RMTD contribution to the relaxation is described by power-law frequency dependence. In the **1**/EG gels the exponent is equal to 0.5 for all gelator concentrations suggesting the equipartition of the diffusion modes with different wavelengths. In this gel the relaxation dispersion data were transformed to a susceptibility representation and a "master-like" curve was constructed. In the **1**/PG gel the exponent varies in the function of gelator concentration. Different behavior of the relaxation dispersion shape is due to the relative sizes of the ordered (at surface) and bulk-like phase. In **1**/EG gel the surface layer of the ordered molecules is always much smaller than the dimension of the gel cavities whereas it differs in **1**/PG gel as a consequence of the disruption of the PG aggregates due to the solvent-gelator interaction.

1 Introduction

Physical, also known as molecular, gels are formed by low molecular mass gelators (LMOGs) and organic solvents or water. The formation of these gels is a result of noncovalent interactions mainly between gelator-gelator but interactions between gelator-solvent and solvent-solvent molecules can also play an important role. Only a well-balanced combination over these interactions leads to the gel formation. Otherwise, an unpredictable competition between crystallization and gelation phenomena occurs. The noncovalent interactions such as hydrogen bonding, π–π stacking, van der Waals and electrostatic interactions, coordination, or charge transfer lead to the self-assembly of the gelator molecules into fibres and to physical entanglement of the fibres, which creates a 3D network, which finally adsorbs the solvent into its structure.[1,2] The physical gels are thermoreversible and, depending on the molecular structure of the LMOG and the solvent which is rigidified, it is possible to form nanoscale superstructures such as nanofibres, nanoribbons, nanosheets, nanoparticles, helical windings, etc. Some of these gels have an ability to alter their function in direct response to environmental conditions such as temperature, light, pH, electromagnetic field, mechanical stress and/or chemical stimuli. They are promising materials for bottom-up nanofabrication tools in various fields, including the transport and release of drugs, foods, catalysis, membranes, sensors, cosmetics, and environmental correction.[1,2]

Molecular gels, are the subject of an ever increasing number of studies not only because they are very attractive for applications in various areas but also because of the fundamental challenges that they raise.[1-8] One of a major challenges today is the role of the solvent after a gel formation and rational design of small size molecular gelators coupled with an understanding of the mechanism of gelation. Prediction of the gelling ability of a compound is not straightforward and thus many gels are still found by serendipity rather than rational design.

Extensive studies of molecular gels have improved the understanding of the self-organization of gelator molecules into a three-dimensional network structure, the gelation phenomenon, the dependence of the thermal stability and of gel morphology on the gelation solvent.[1-16] Surprisingly, not many papers are devoted to the molecular dynamics of solvents in molecular gels.[16-22] Molecular gels can be treated as porous materials in which the solvent molecules are confined in pores (cavities) of a rigid matrix. It is well established for polar and nonpolar liquids filled in porous media or liquids adsorbed on the surface of porous glasses or fineparticle agglomerates that spatial restriction and interactions with surfaces (adsorption) significantly influence the molecular dynamics of a liquid.[23] A slowing down of the molecular motions which are characterized by the correlation time up to 8 orders of magnitude greater than in the bulk liquids is observed and the molecules tend to be oriented by the surface. On the other hand, translational diffusion is comparatively fast, within an order of magnitude of the bulk value.[23-25] The observed very long correlation times (10^{-4} to 10^{-6} s) of confined liquids was successfully explained assuming that the dominating NMR relaxation mechanism of liquids interacting with internal surfaces of porous materials is reorientations mediated by translational displacements (RMTD).[26]

The field-cycling relaxometry[24,27,28] is the NMR method most suitable for the identification and characterization of molecular dynamics in porous media and at liquid-solid interfaces. With the aid of this method one can measure a frequency dependence of spin-lattice relaxation time T_1 which reflects the features of the spectral density function and, hence, of the dipolar correlation function. With commercially accessible spectrometer this method covers a broad frequency range from a few kHz to 40 MHz. Different contributions of the molecular motions to the overall relaxation dominate at different frequency ranges and therefore can be identified. The fast rotational motions dominate in the frequency regime

above MHz whereas the slow motions like the molecular reorientation mediated by translational diffusion dominate at kHz frequency.

The RMTD mechanism of relaxation was till now justified for liquids confined in nanometer-scale pores with the aid of the field-cycling relaxometry.[23,24] In the present paper we will shown that this mechanism also occurs for liquids confined to matrices of molecular gels but only for those containing polar surfaces in combination with polar adsorbates.

Contrary to previous relaxometry studies[16,20,21] where only the weak solvent-gelator interactions were indicated, in this paper we present for the first time a quantitative analysis of proton spin-lattice relaxation dispersion of solvents for a strong case of interactions observed in molecular gels. The studied gels are composed by LMOG 4,6,4',6'-O-Terephthylidene-bis(methyl α-D-glucopyranoside) (**1**) with ethylene glycol (EG) and 1,3-propanediol (PG). The gelator is composed of two glucopyranoside units linked to a benzene core. The surface of the gel matrix formed by gelator **1** molecules is polar due to OH groups of sugar molecules and thus can interact with polar EG and PG solvents. The chemical structures of both solvents are closely related but as shown in the previous paper[16] they formed with **1** gels which differed as to the thermal stability, types of aggregates self-assembled during gel formation, gel microstructure, and solvent diffusivity. In present studies we will show that the spin-lattice relaxation of both solvents measured in the function of gelator concentration also behaves differently.

The main purpose of the present work is to study the proton spin-lattice relaxation mechanisms of the solvent in the **1**/EG and **1**/PG gels, the surface induced order and its impact on the solvent dynamics. The measurements were performed in the function of Larmor frequency, using field-cycling relaxometry method, at different gelator concentrations. The studies gave us the opportunity to study the rotational and translational diffusion of the bulk-like solvents inside the pores as well as the surface diffusion dynamic. The latter one is the

crucial process of the RMTD, mechanism of the spin-lattice relaxation which served for the interpretation of the spin-lattice relaxation data of confined solvents in the low frequency range.

The studies presented in this paper have shown that RMTD mechanism of relaxation is suitable for the interpretation of relaxation data for solvent immobilized in molecular gels. Moreover, they also experimentally proved the solvent-gelator interactions after the gel formation, which up until now were considered questionable.

2 Experimental section

2.1 Materials and gel preparation

4,6,4',6'-O-Terephthylidene-bis(methyl α-D-glucopyranoside) – gelator **1**, was synthesized according to the procedure described previously.[26] Ethylene glycol (EG) and 1,3-propanediol (PG) for gels preparation were provided by Sigma-Aldrich and used without further purification. The gels were prepared from mixtures of powdered gelator **1** and a proper solvent under different weight concentrations of gelator ranging from 0.5 to 4 wt% via a thermal heating-cooling cycle, which allows the formation of the noncovalent interactions responsible for the gel network. Upon cooling below a characteristic temperature T_{gs}, the sol is converted into an elastic gel that can hold its weight under the "tube inversion test."

2.2 NMR relaxometry measurements

The proton spin-lattice relaxation time, T_1, of confined solvents and in the bulk state have been measured in a function of Larmor frequency and gelator concentration with the commercial fast field-cycling NMR relaxometer (Spin Master FFC 2000, Stelar Mede, Italy). The measurements were performed in the frequency range from a few kilohertz to 25 MHz. The sample was initially polarized in the polarization magnetic field B_{POL} = 0.625 T for a time

$t_{POL} > 5T_1$. The sequence B_{POL} - B_L - τ - B_{ACQ} - $\pi/2$-FID was applied, where τ is the evolution time, $\pi/2$ is the radio-frequency pulse, and B_L and B_{ACQ} are correspondingly the relaxation and acquisition magnetic fields. The switching time between applied magnetic fields was equal to 3 ms. Performing the experiment in the function of τ permits for determination of the spin-lattice relaxation time $T_1(B_L)$, i.e., $T_1(\omega = \gamma B_L)$. The plot of the relaxation rate $R_1(\omega)$ ($R_1 = 1/T_1$) vs Larmor frequency is called the nuclear magnetic resonance dispersion (NMRD). The time dependence of the magnetization curves was a monoexponential function over three decades of time and for all gelator concentrations. The magnetization measured in the gels comes only from the solvent protons because the contribution of the gelator protons, which form a rigid matrix in the gel phase with strongly restricted motion, is undetectable under the applied NMR measuring conditions. Because of the low resolution of field-cycling NMR relaxometry measurements and the inhomogeneity of magnetic field, the resonances of OH and CH_2 groups of PG and EG solvents totally overlapped. The measurements were performed at 290 K corresponding to the gels phase. The temperature of the sample was controlled by the Stelar VCT unit and stabilized within ± 0.01 K accuracy. The experimental error of spin-lattice relaxation measurements was estimated to be less than ± 2 %. The gelator concentration in studied gels varies from 0.5 to 4 wt%.

2.3 Microscopic observation

The gel microstructures were taken by an Olympus BX53 microscope (Japan) and Olympus Stream START software used for recording and analyzing obtained images. The configuration of the system allowed for observation with the use of phase contrast mode, differential interface mode and polarizing mode which allowed visualizing molecular aggregates of the gelator. The images were obtained for a gel sample carefully cast on the

microscopic slides covered with 130 μm coverslip and immediately subjected to microscopic observations.

3 Relaxation mechanisms

3.1 Dipole-dipole interactions

The intramolecular and intermolecular dipole-dipole interaction, respectively modulated in time by molecular rotation and relative translational diffusion of molecules under study, is the main spin-lattice relaxation mechanism of equivalent spins of the quantum number ½ (protons in our case) in diamagnetic systems.[30] The rotational motion leads to the fluctuations of the orientation of the vector connecting the interacting spins within the same molecule with respect to the direction of the external magnetic field. The relative translational diffusion of the molecules modulates not only the orientation of the vector connecting the interacting spins located on different molecules but also changes its distance. Assuming that the rotational and translational motions are stochastically uncorrelated, the intramolecular and intermolecular dipole-dipole interaction additively contribute to the measured spin-lattice relaxation, described by a relaxation rate R_1 ($R_1 = 1/T_1$):[30]

$$R_1(\omega) = R_{1\,intra}(\omega) + R_{1\,inter}(\omega), \quad (1)$$

where ω is the Larmor frequency ($\omega = \gamma B_L$, γ is the gyromagnetic ratio). $R_{1,intra}$ and $R_{1,inter}$ describe the contribution to the relaxation originating from dipolar spin interactions within or between the molecules, respectively, which are expressed in terms of spectral density functions.[31] The density function $J(\omega)$ is given as the Fourier transform of the correlation function $G(t)$ describing the fluctuations of the dipolar Hamiltonian, which induce the spin transitions. The transition's probability per time unit is proportional to the spectral density

function and for single and double quantum transitions is directly reflected by the measured spin-lattice relaxation rate of equivalent spins:[31]

$$R_{1,i}(\omega) = C_i[J_i(\omega) + 4J_i(2\omega)]. \quad (2)$$

In eqn (2) i stands for an intramolecular or intermolecular contribution, C_i is the effective dipole-dipole constant, and $J_i(\omega)$ is the spectral density function. C_{intra} is described by:

$$C_{intra} = \left(\frac{\mu_0}{4\pi}\right)^2 \frac{2}{5} I(I+1) \frac{1}{N} \left(\gamma^2 \hbar \sum_{i,j=1}^{N} r_{ij}^{-3}\right)^2, \quad (3)$$

where h is Planck's constant, I is the spin number (I=1/2 for protons), μ_o is the permeability of the vacuum, γ is the gyromagnetic ratio, and r is the distance between a reference spin and the ith spin in the assembly of the N spins within the molecules, the summation goes over all spins in the molecule. For simple liquids, the density function $J_{intra}(\omega)$ for the rotational diffusion modulating the intramolecular dipole-dipole coupling is usually expressed in the Lorentzian form[31] but for viscous liquids it is more appropriate[32] to assume a Cole-Davidson form[33] of this function:

$$J_{intra}(\omega) = \frac{\sin[\beta \arctan(\omega\tau)]}{\omega[1 + (\omega\tau_{CD})^2]^{\beta/2}}. \quad (4)$$

The parameter β ($0 < \beta \leq 1$) reflects the distribution of the correlation time describing the rotational motions in viscous liquids (for β =1 the function becomes Lorentzian). The constant τ_{CD} is related to the rotational correlation time τ_{rot} by the following relation: $\tau_{rot} = \beta\tau_{CD}$. The form of the spectral density function, $J_{inter}(\omega)$ for translational diffusion modulating the intermolecular dipole-dipole coupling, depends on the model assumed. The one frequently used is the so-called force-free-hard-sphere (FFHS) diffusion model[30-36] It is based on the assumptions that the interacting spins are located at the center of molecules that are treated as a hard spheres and the translational motions are correctly described by Fick's diffusion

equation with proper boundary conditions where d is a distance of the closest approach, which is of an order of the molecule size. The C_{inter} constant in the FFHS model is described by:

$$C_{inter} = \frac{2}{5} I(I+1) \left(\frac{\mu_0}{4\pi} h\gamma^2 \right)^2 \frac{4\pi}{3} \left(\frac{N}{d^3} \right), \quad (5)$$

where $\frac{4\pi}{3}\left(\frac{N}{d^3}\right)$ is the number of spins per unit sphere and d is the distance of the closest approach of interacting spins. The intermolecular spectral density function in the FFHS model is given as:

$$J_{inter}(\omega) = 72 \frac{3}{4\pi} \int_0^\infty \frac{u^2}{81 + 9u^2 - 2u^4 + u^6} \times \frac{u^2 \tau_{trans}}{u^4 + (\omega \tau_{trans})^2} du \,, \quad (6)$$

where u is the integration variable and the translational correlation time τ_{trans} is defined as: $\tau_{\text{trans}} = d^2/D_{12}$ and D_{12} is the relative translational diffusion coefficient.

The intermolecular dipolar interactions for bulk liquids tend to fluctuate much slower than intramolecular couplings. The reason is that the time modulation of the former interaction is governed by translational Brownian motions of the whole molecules over the distance considerably exceeding the dimensions of the molecule whereas the latter one by rotational diffusion about molecular axes.

The situation become different as soon as liquid molecules are adsorbed on an surface of pores and an additional spin-lattice relaxation mechanism (or relaxation dynamical process) called reorientation mediated by translational displacements (RMTD)[23-26] starts to play a role. As a consequence of the liquid-pore surface interactions the adsorbed molecule tends to be oriented in a preferential direction relative to the local surface and executes about this orientation rotational diffusion comparable to that in bulk but hindered and incomplete because of the surface. Consequently, this reorientation does not totally average out the intramolecular spin interactions and causes a fast drop of the correlation function only to some residual value. The intramolecular interaction is further modulated in time by

translational displacement of the molecules along a rough and shaped pore surface with different local orientations. As a result of this displacement the adsorbed molecule changes its orientation according to the surface contour and to the external magnetic field B_o. Such molecular reorientations mediated by translational displacements of the molecules occur on a much slower time scale than bulk rotational or translational diffusion. This dynamical process known as RMTD is an efficient relaxation mechanism extending the orientation correlation times while maintaining the translational mobility. The RMTD becomes effective at low frequencies and was successfully applied to explain the extraordinarily long correlation times (10^{-4} - 10^{-7} s) observed for liquids or liquid crystals confined to porous media, ionic liquids in polymer matrix, or molecules adsorbed on surfaces of macromolecules or particle aggregates.[23-26,37-41] In such systems molecular translational diffusion despite the fact that it modulates intermolecular spin interactions, additionally modulates intramolecular proton spin interactions via the RMTD mechanism. RMTD requires polar surface and adsorbate molecules but without specific chemical bonding sites on the surfaces. The displacement of the molecules along the surface is executed by translational diffusion which can be the surface diffusion in the proper sense (weakly adsorbing system) or bulk mediated surface diffusion[40] (BMSD) (strongly adsorbing system). In the latter case many acts of adsorption and desorption events occur before molecules are finally released to the bulk.

For normal surface diffusion the probability density for the displacement r in time t is described by Gaussian form and can be analyzed in terms of modes with wave numbers q. The spectral density function $J_k(\omega)_{RMTD}$ required for the calculation of T_1 contains the Lorentzian-type contribution of all q modes, weighted by the orientational structure factor $Q(q)$, which depends on the surface structure. The $J_k(\omega)_{RMTD}$ in the interval between q_{min} and q_{max} is thus expressed as:

$$J_k(\omega)_{RMTD} = \int_{q_{\min}}^{q^{\max}} Q(q)\ \frac{2\tau_q}{1+(\omega\tau_q)^2}\, dq\,, \tag{7}$$

where $\tau_q = (Dq^2)^{-1}$ is the characteristic time, which described the exponential decay of the orientational correlation function for the diffusion mode with the wave number q, and D is the diffusion coefficient. Eqn (7) links dynamics properties of adsorbate molecules with structural details of the adsorbent surface.

Within the assumption that in the range between $q_{\min}$ and $q_{\max}$ all modes are equally weighted the relaxation rate induce by RMTD is given by:[23,26,37-41]

$$R_{1RMTD}(\omega) = A_{RMTD}\left\{\frac{1}{\omega^{1/2}}\left[f\left(\frac{\omega_{RMTD\max}}{\omega}\right) - f\left(\frac{\omega_{RMTD\min}}{\omega}\right)\right] + \frac{4}{(2\omega)^{1/2}}\left[f\left(\frac{\omega_{RMTD\max}}{2\omega}\right) - f\left(\frac{\omega_{RMTD\min}}{2\omega}\right)\right]\right., \tag{8}$$

with

$$f(w) = \arctan\left(\sqrt{2w}+1\right) + \arctan\left(\sqrt{2w}-1\right) - \arctan h\left(\frac{\sqrt{2w}}{w+1}\right), \tag{9}$$

and $\omega_{\mathrm{RMTDmin}} = Dq^2_{\min}$, $\omega_{\mathrm{RMTDmax}} = Dq^2_{\max}$. In eqn (8) the constant A_{RMTD} depends on the residual dipole-dipole proton interaction which is averaged by local molecular orientations, on the microstructural features of the confined matrix, on the diffusion coefficient and on the fraction of the molecule at the surface. The low frequency cut-off $\omega_{\mathrm{RMTDmin}}$ determines the "inflection point" where $R_{1\mathrm{RMTD}}$ (ω) levels off into a frequency independent plateau. The corresponding $\tau_{\mathrm{RMTDmax}} = 1/\omega_{\mathrm{RMTDmin}}$ is the slowest decay of orientational correlation function characterizing the diffusion along the mode with wave number $q_{\min}$. The relaxation rate $R_{1\mathrm{RMTD}} \propto \omega^{-0.5}$ behavior predicted by eqn (8) in the range between $\omega_{\mathrm{RMTDmin}}$ and $\omega_{\mathrm{RMTDmax}}$ is characteristic for an equipartition of wave numbers describing different modes ($Q(q)$ = const). Generally this factor is a complex function of the wave number. For specific q dependence $Q(q) = cq^{-\chi} + e$ (c and e are constants independent of q)[39] the $R_{1\mathrm{RMTD}} \propto \omega^{-p}$ with parameter p of different value than 0.5.

3.2 Total relaxation rates

The spin-lattice relaxation of liquids confined to porous media is usually evaluated assuming the two-phase fast-exchange model where some of the molecules at the surface formed one phase and the other molecules within the cavities which behave like bulk molecules formed the second one. The exchange is defined by an effective exchange time τ_{ex} which characterize the exchange kinetics between two phases and can be rated fast or slow depending on the reference time scale. The exchange is fast when referenced to the time scale of the spin-lattice relaxation time but normally slow with reference to the RMTD process.[41,42] With the assumption that the RMTD process is much faster than the exchange process, the measured effective relaxation rate $R_{1\mathrm{eff}}$ is described by two contributing phases: bulk-like, $R_{1\mathrm{bulk}}$, and surface (adsorbate), $R_{1\mathrm{RMTD}}$ phase and given by eqn (12). The contribution of the exchange mechanism is minor in the low frequency range and can be omitted[41,42]

$$R_{1eff}(\omega) = R_{1bulk}(\omega) + R_{1RMTD}(\omega) \qquad (12)$$

The $R_{1\mathrm{bulk}}$ in eqn (12) is described by eqn (1) and $R_{1\mathrm{RMTD}}$ by eqn (8) or in the frequency range between $\omega_{\mathrm{RMTDmin}}$ and $\omega_{\mathrm{RMTDmax}}$ by relation: $R_{1\mathrm{RMTD}} \propto \omega^{-p}$.

4 Results and discussion

4.1 Gels microstructure

The microscopic observations of **1**/EG and **1**/PG gel microstructures were performed not for xerogels but for wet gels with PG and EG solvents still trapped inside gel matrices. Despite the similarity of the solvents they formed a different microstructure in gels with **1**. Representative micrographs are shown in Fig. 1. The matrix of **1**/EG gel changes its microstructure with gelator concentration. For 0.5 wt% (not shown) and 2 wt% (Fig. 1a) the matrix consists of bending fibers which formed more or less closed circles determining the

large cavities filled with EG solvent. When increasing the gelator concentration to 4 wt% the matrix additionally contains the bundles of crossing fibres with different lengths, and orientations, dispersed in the gel (Fig. 1b). The matrix of **1**/PG gel for 4 wt% gelator concentration shown in Fig. 1c is much more regular and appears like a honeycomb. Such supermolecular network clearly depicts the better entrapment of the solvent molecules as compared to the **1**/EG gel.

4.2 Solvent-pore surface interactions reviled by dispersion of the solvent spin-lattice relaxation time

The confinement of liquids in the cavities of porous media influences their NMR relaxation behavior. The origin of this effect is due to the geometrical restriction imposed by porous media on the confined liquid molecules or liquid–pore surface interactions. In the matrices of the studied gels, as shown in Fig. 1, the pores are in the order of tens of micrometers and are large enough to not show the significant geometrical restriction effects. Consequently, any effect observed on the spin-lattice relaxation data of solvent in gel as compared to corresponding bulk solvent is mainly due to the solvent-pore surface interactions.

The NMRD profiles of ethylene glycol in **1**/EG gel and of 1,3-propanediol in **1**/PG gel, obtained at different gelator concentrations, are shown in Figs. 2a and 2b, respectively. Both solvents differ as to the value of the relaxation times. It is mainly a consequence of the viscosity. The larger viscosity of PG solvent means slower molecular motions, stronger dipole-dipole couplings and consequently shorter T_1 (or longer R_1) as compared to EG solvent. Slower dynamics of PG causes also a shift of the frequency at which the maximum dispersion occurs to a lower value as compared to EG. This dispersion starts to be seen at about 10 MHz for PG but for EG is not pronounced in the studied frequency range. The most important result shown in Figs. 2a and 2b concerns the shape of the NMRD profiles of

confined solvents. They are significantly different as compared to the bulk. The relaxation rates of bulk PG and EG solvents are frequency independent in the low frequency region below 1 MHz whereas a broad and pronounced dispersion region appears in R_1 for PG and EG in the gel phase. The R_1 of confined EG smoothly increases with decreasing frequency until it reaches a plateau at about 0.01 MHz, well pronounced for larger gelator concentrations. A similar behavior is also observed for confined PG but without reaching a plateau in the studied frequency range. The observed low-frequency dispersion of the R_1 is a consequence of a specific solvent-inner pore surface interaction which is a base of the RMTD, an additional relaxation mechanism active in the low frequency range but only for confined solvents. The RMTD leads to the shortening of the spin-lattice relaxation time of solvent protons confined in gel as compared to the bulk solvent. As a result the low-frequency dispersion is observed.

The solvent-pore surface interaction differs for EG and PG solvents as reflected by the dispersion behavior in the function of gelator concentrations. For **1**/EG gel amplitude of the dispersion continuously increases as a function of the gelator concentration (see Fig. 2a). The higher concentration leads to the larger matrix surface and consequently to the increase of the efficiency of the solvent-pore surface interaction. For **1**/PG the continuous increase of the amplitude of dispersion is observed only up to 1.5 wt% followed by a small decrease of the dispersion for 2 wt% gel and finally almost no dependence on the concentration is observed for gels with higher concentrations. Such behavior is somewhat confusing. As an explanation we assumed that for **1**/PG gel the solid matrix can develop only to some extent. Above a particular gelator concentration of 2 wt %, the gelator molecules are not forming a further gel matrix but are interacting with PG aggregates leading to their disruption. Thus, the microstructure of the gel matrix remains unchanged but the size of the solvent aggregates decreases.

In order to extract the relaxometry data connected to the solvent-pore surface interaction from the measured effective spin-lattice relaxation times of confined EG and PG shown in Fig. 2a and Fig. 2b, the full analysis of the relaxometry data for bulk solvent is necessary.

4.2.1 Proton spin-lattice relaxation of bulk solvents

The influence of translational diffusion on the spin-lattice relaxation time can usually be neglected for low-molecular mass liquids like EG or PG because in the whole frequency range the relaxation is dominated by the intramolecular interaction. However, it is known that these solvents formed in bulk the aggregates of different sizes and shapes through the network of hydrogen bonds.[43,44] Hence, it is reasonable to assume that they are characterized by a strong motional anisotropy and consequently the intermolecular dipole-dipole interaction, in addition to the intramolecular one, becomes an important contribution to the effective relaxation time. Therefore, eqn (1) was used for the interpretation of NMRD profiles of bulk EG and PG solvents with the rotational contribution described by a Cole-Davidson spectral density function given by eqn (4) and the translational one derived from the FFHS model and described by eqn (6). Results of the fit of eqn (1) to experimental data are presented as the solid lines in Fig. 3a and Fig. 3b for EG and PG, respectively. These figures also included the intramolecular (dashed lines) and intermolecular (doted lines) contributions to the overall relaxation. The most important fitted parameters are the correlation times. The rotational correlation times τ_{rot} are equal to 9.0×10^{-10} s for EG and 1.5×10^{-9} s for PG. The parameter β is correspondingly equal to 0.94 and 0.90. These values are close to 1 but fits with Lorentzian function were not satisfactory. The translational correlation time τ_{trans} is equal to 1.3×10^{-8} s, and 3.7×10^{-8} s, for EG and PG, respectively. With the relation $\tau_{trans} = d^2/D_{12}$, the fitted τ_{trans} values, and self-diffusion coefficients D $(D_{12}=2D)$ measured by pulse gradient spin echo method [22] (5.7×10^{-11} m^2/s for EG and 2.2×10^{-11} m^2/s for PG) we could estimate the parameter

d, which is supposed to be equal to the dimension of the molecule. The obtained values are 70 and 13 Å for EG and PG, respectively. The dimension of the EG molecule is about 3.5 Å and of the PG molecule about 4.5 Å. Therefore, the obtained values of *d* reflect the average dimensions of the aggregates formed by EG and PG molecules via hydrogen bonding interaction and prove the aggregation nature of these solvents.

4.2.2 Proton spin-relaxation of solvents confined in gels

The proton relaxation rate of EG and PG solvents confined in the gels matrix formed by low molecular mass gelator **1** (data presented in Fig. 2a and Fig. 2b) is induced by fast molecular motions and by a slow dynamic process. Their time scales differ by several orders of magnitude and can be treated independently. Therefore, we applied eqn (12) where $R_{1\mathrm{bulk}}$ and $R_{1\mathrm{RMTD}}$ represent the contribution of fast motions and of the slow dynamic process, respectively. As suggested by data given in Fig. 2, the relaxation rate originating from fast motions can be identified with the relaxation rate measured in bulk solvents. With the aid of the analysis of bulk solvents relaxometry data we can obtain the contribution to the measured effective relaxation rate, $R_{1\mathrm{eff}}$, resulting from RMTD process. For this purpose, the corresponding values of the bulk solvents $R_{1\mathrm{bulk}}(\omega)$ (solid lines in Figs. 3) were subtracted from the measured values $R_{1\mathrm{eff}}(\omega)$ of the confined solvents shown in Figs. 2. The examples of the obtained results are given in Fig. 4a and Fig. 4b for **1**/EG and **1**/PG gel, respectively. The R_{RMTD} contributions are presented as open symbols, the corresponding $R_{1\mathrm{eff}}$ by closed symbols and the contribution from $R_{1\mathrm{bulk}}$ by the dashed lines. From Fig. 4a, it is seen that for confined EG solvent at least two dispersion regions can be distinguished: at lowest frequencies accessible a plateau is reached and in the intermediated frequency, where RMTD mechanism is expected to dominate, the relaxation rate dispersion is described by power law.

The crossover from the power law regime of the dispersion to the low-frequency plateau indicates the condition $\omega\tau_{RMTDmax} = 1$. Thus, for confined EG solvent the longest correlation time $\tau_{RMTDmax}$ related to the RMTD process is of the order of 10^{-5} s. In the case of confined PG solvent only an intermediated dispersion region is observed. The low-frequency plateau is not reached because it is shifted behind the lowest frequency measured. Therefore, we can predict that the longest correlation time related to the RMTD process for confined PG is longer than that observed for EG, *i.e.*, $\tau_{RMTDmax} > 10^{-5}$ s.

The power law describing the RMTD dispersion, $R_{1RMTD} \propto \omega^{p}$, is observed for both gels over three decades of the frequency. In the **1**/EG gel, for all studied gelator concentrations, the R_{1RMTD} is well characterized by the exponent $p = 0.50 \pm 0.05$. However, as seen in Fig. 4, for 3 wt% gel (also for 2.5, 3.5 and 4 wt%), additional slope of the R_{1RMTD} ($p = 0.81$) can be distinguished in the intermediated frequency range. In order to visualize the changes in the relaxation of confined EG due to gelator concentration, the obtained relaxation dispersion data were transformed to a susceptibility representation according to the relation: $\chi''(\omega) = \omega R_{1RMTD}(\omega)$.[45,46] Next, the susceptibility results for each of gelator concentrations were combined (properly shifted along the frequency axis and replotted versus $\omega\tau$) in order to construct a "master-like" curve, as shown in Fig. 5. The NMR susceptibility curves corresponding to different gelator concentrations well coincide because their shape remains unchanged with gelator concentration and is described by the exponent $p = 0.5$. Additional contributions to the R_{1RMTD} with slope different than 0.5 is seen well in the insert in Fig. 5. In **1**/PG gel the situation is different and the R_{1RMTD} changes its slope in a function of gelator concentrations but for particular concentration is characterized only by one p value as shown in Fig. 6. Therefore, the attempt to construct the "master-like" curve was unsatisfactory.

The intensity function describing the RMTD process contains the structural factor and dynamics part as given by eqn (7). Consequently, spin-lattice relaxation caused by RMTD is

the combined result of molecular dynamics and of the surface structure. The power law dependence of the relaxation rate results from the assumption of normal surface diffusion described by Gaussian propagator[47] and it was found to occur for studied gels for all gelator concentrations. Thus, for identical propagator for normal diffusion the different shape of R_{1RMTD} dispersion directly visualizes the different surface geometries. This suggests that the geometrical features of the surfaces on which the RMTD process takes place in **1**/EG and **1**/PG gels are not the same irrespective of the fact that chemically the surfaces are the same, composed by the same gelator **1**. Therefore, a different orientational structure factor, $Q(q)$, has to appear dispite the fact that the same propagator is taken into consideration. For confined EG the relaxation rate dispersions are well described by the power law with the exponent p = 0.5 suggesting the equipartition of the diffusion modes with different wave numbers, *i.e.*, $Q(q)$ = const. This factor is probably a complex function of the wave number for **1**/PG gel because the relaxation dispersion of confined PG is described by the power low with $p \neq 0.5$ and the p parameter depends on the gelator concentrations.

The RMTD dispersion slope, as shown by Monte Carlo simulations[47], also depends on the relative sizes of the width of the surface layer, δr, formed by the ordered molecules at the pore surface and dimension of the pore, R, filled with bulk-like molecules. A thinner layer tends to produce a flatter slope. Thus, interpreting our experimental results we can conclude that PG at the pore surface formed a thinner layer as compared to the EG. With the assumption that the width of the surface layer corresponds to the dimension of the aggregates, this conclusion agrees with previously calculated dimensions of aggregates formed by PG and EG molecules, which are correspondingly equal to 13 and 70 Å. The Monte Carlo simulation[45] also showed that if the width δr is much smaller than R, then the differences in the slopes are minor. Such a situation takes place in the **1**/EG gel where one slope of the dispersion curve is observed for all gelator concentrations. The appearance of an additional slope observed for this gel with

concentration above 2.5 wt% is due to the changes of the gel matrix as shown in Fig. 1a (for 2 wt%) a nd Fig. 1b (4 wt%). For a gel with higher concentrations in addition to large cavities like that occurring in 2 wt% gel also smaller one are seen in the matrix. The EG aggregates are not disrupted when interacting with the pore surface.[22] Thus, it is reasonable to assume that they form in the smaller pores, the surface layer of the same width as in the larger one. However, in this case δr is no longer much smaller than R. Additionally also the shape of smaller pores is different as compared to larger one and consequently a steeper slope of the relaxation rate dispersion is observed. The change of the slope of the relaxation dispersion observed in **1**/PG gel is a consequence of solvent-pore surface interaction[22] unlike than in **1**/EG gel and much smaller pores than in **1**/EG gel (Fig.1c). The surface matrix of **1**/PG gel develops only up to 2 wt% of gelator concentration. Further increase of gelator concentration leads only to the disruption of PG aggregates.[22] Consequently, the microstructure of the gel matrix remains unchanged but the size of the solvent aggregates decreases. Therefore, the relative sizes of the surface ordered and the bulk-like phase vary for all concentrations and different slopes of the $R_{1\mathrm{RMTD}}$ are observed.

Conclusion

The purpose of the present work was to study the proton spin-lattice relaxation mechanisms of solvent in the gels, the surface induced order and its impact on the solvent dynamics. The experimental relaxometry data clearly shows differences between the spin-lattice relaxation dispersion of bulk and confined solvents. The bulk relaxation rates show the dispersion only in the MHz frequency range whereas the relaxation dispersion of confined EG and PG solvents in the gels of **1** show the pronounced dispersion in the kHz region. Therefore, we concluded that the interaction of solvent molecules with the gel matrices introduce additional

relaxation mechanism, RMTD, not found in the bulk solvents. Only this mechanism can explained the long correlation time of the order of 10^{-5} s obtained for confined EG molecules and even longer for PG molecules. To the best of our knowledge this is the first evidence of RMTD relaxation mechanism in gels composed of LMOGs with organic solvents. The gels are composed by polar solvents and interact with polar surface of gelator **1.**

Acknowledgments

Financial support for this work from t**he National Centre for Science (Grant** N N202 1961 40) is gratefully acknowledged.

References

1 P. Terech and R. G. Weiss, *Molecular Gels: Materials with Self-Assembled Fibrillar Network*s, Springer, Dordrecht, The Netherlands, 2006.

2 X. Y. Liu, J.-L. Li, Soft Fibrillar Materials, Fabrication and Applications, Wiley-VCH, Weinheim, Germany, 2013.

3 J. W. Steed, *Chem. Commun*., 2011, **47**, 1379.

4 M. O. M. Piepenbrock, G. O. Lloyd, N. Clarke and J. W. Steed, *Chem. Rev.*, 2010, **110**, 1960.

5 M. Llusar and C. Sanchez, *Chem. Mater*., 2008, **20**, 782.

6 N. M. Sangeetha and U. Maitra, *Chem. Soc. Rev*., 2005, **34**, 821.

7 S. Samai, J. Dey and K. Biradha, *Soft Matter*, 2011, **7**, 2121.

8 Z. Xu, J. Peng, N. Yan, H. Yu, S. Zhang, K. Liu and Y. Fang, *Soft Matter*, 2013, **9**, 2121.

9 F. Allix, P. Curcio, Q. N. Pham, G. Pickaert and B. Jamart-Gregoire, *Langmuir*, 2010, **26**, 16818.

10 J. Tritt-Goc, M. Bielejewski, R. Luboradzki and A. Łapinski, *Langmuir*, 2008, **24**, 534.

11 M. Bielejewski, A. Łapiński, R. Luboradzki and J. Tritt-Goc, *Langmuir*, 2009, **25**, 8274.

12 J. Makarevic, M. Jokic, M. Peric, V. Tomisic, B. Kojic-Prodic and M. Zinic, *Chem.–Eur. J.*, 2001, **7**, 3328.

13 G. Zhu and J. S. Dordic, *Chem. Mater*., 2006, **18**, 5988.

14 A. R. Hirst and D. K. Smith, *Langmuir*, 2004, **20**, 10851.

15 W. Edwards, C. A. Lagadec and D. K. Smith, *Soft Matte*r, 2011, **7**, 110.

16 M. Bielejewski, J. Kowalczuk, J. Kasńska, A. Łapiński,R. Luboradzki, O. Demchuk, J. Tritt-Goc, *Soft Matter*, 2013, **9**, 7501.

17 M. Yemloul, E. Steiner, A. Robert, S. Bouguet-Bonnet, F. Allix, B. Jamart-Gregoire and D. Canet, *J. Phys. Chem. B*, 2011, **115**, 2511.

18 E. Steiner, S. Bouguet-Bonnet, A. Robert and D. Canet, *Concepts Magn. Reson., Part A*, 2012, **40**, 80.

19 J. Kowalczuk, S. Jarosz and J. Tritt-Goc, T*etrahedron*, 2009, **65**, 9801.

20 M. Bielejewski and J. Tritt-Goc, *Langmuir*, 2010, **26**, 17459.

21 M. Bielejewski, A. Łapinski, R. Luboradzki and J. Tritt-Goc, *Tetrahedron*, 2011, **67**, 7222.

22 J. Kowalczuk, M. Bielejewski, A. Łapinski, R. Luboradzki, and J. Tritt-Goc, *J. Phys, Chem. B*, 2014, **118**, 4005.

23 R. Kimmich, *Principles of Soft-Matter Dynamics: Basic Theories, Non-invasive Methods, Mesoscopic Aspects,* Springer Dordrecht, Heidelberg, 2012.

24 R. Kimmich and E. Anoardo, *Prog. Nucl. Magn. Reson. Spectrosc*., 2004, **44**, 257.

25 S. Staph and R. Kimmich, *Chem. Phys. Lett*., 1997, **275**, 261.

26 R. Kimmich and H. W. Weber, *Phys. Rev. B*, 1993, **47**, 11788.

27 F. Noack, *Prog. Nucl. Magn. Reson. Spectrosc*., 1986, **18**, 171.

28 E. Anoardo, G. Galli, G. Ferrante, *Appl. Magn. Reson.,* 2001, **20**, 365.

29 J. Maślińska-Solich, *Macromol. Biosci.* 2001, **1**, 312.

30 A. Abragam, *The principles of nuclear magnetism*, Oxford University Press, Oxford, United Kingdom 1961.

31 N. Bloembergen, E. M. Purcell, R. V. Pound, *Phys. Rev*., 1948, **73**, 679.

32 D. Kruk, A. Hermman, and E. A. Rossler, *Prog. Nucl. Magn. Reson,* 2012, **63**,33.

33 C. J. F. Bottcher and P. Bordewijk, *Theory of Electric Polarization*, Elsevier, Amsterdam, 1973.

34 Y. Ayant, E. Belorizky, J. Alizon, and J. Gallice, *J. Phys.,* 1975, **36,** 991.

35 L. P. Hwang, J.H. Freed, *J. Chem. Phys*., 1975, **63,** 4017.

35 Y. Ayant, E. Belorizky, P. Fries, and J. Rosset, *J. Phys.*, 1977, **38**, 325.

36 C. F. Polnaszek, R. Bryan, J. *Chem. Phys*., 1984, **81**, 4038.

37 C. F. Martins, L. Neves, I. M. Coelhoso, F. VacaChavez, J. G. Crespo, P.J. Sebastiao, *Fuel Cells,* 2013, **6**, 1166.

38 M. Rajeswari, S. Dhara, K. Venu, V. S. S. Sastry, and R. Dabrowski, *Soft Matter*, 2012, **8**, 10008.

39 M. Vilfan, T. Apih, P. J. Sebastiao, G. Lahajnar, and S. Zumer, *Phys. Rev. E*, 2007, **76**, 051708.

40 O. V. Bychuk and B. O'Shaughnessy, *J. Phys. II,* 1994, **4**, 1135.

41 P. J. Sebastio, D. Sousa, A. C. Ribeiro, M. Vilfan, G. Lahajnar, J. Seliger, S. Zumer, *Phys. Rev. E*, 2005, **72**, 061702.

42 E. Anorado, F. grinberg, M. Vilfan, R. Kimmich, *Chem. Phys*., 2004, **297**, 99.

43 H. L. Tavernier, M. D. Fayer, *J. Chem. Phys.,* 2000, **114***,* 4552.

44 J. A. Padró, L. Saiz, E. Guàrdia, *J. Mol. Structure,* 1997, **416**, 243.

45 S. Kariyo, C. Gainaru, H. Schick, A. Brodin, V. N. Novikov, E. A. Rossler, *Phys. Rev. Lett*., 2006, **97**, 207803.

46 S. R. Meier, D. Kruk, and E. A. Rossler, *ChemPhysChem.,* 2013, **14**, 3071.

47 T. Zawada and R. Kimmich, *J. Chem. Phys.,* 1998, **109**, 6929.

List of Figures

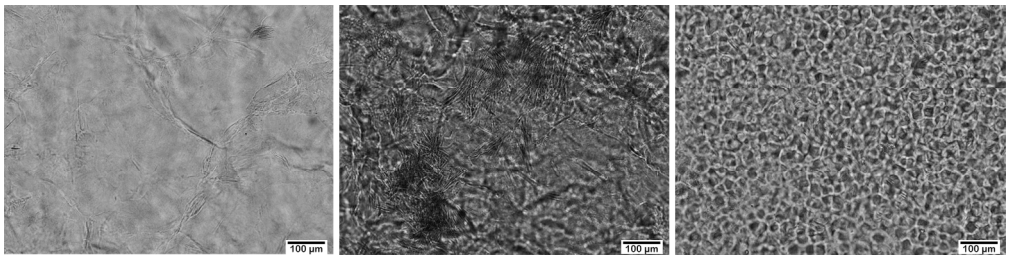

Figure 1
170x42mm (300 x 300 DPI)

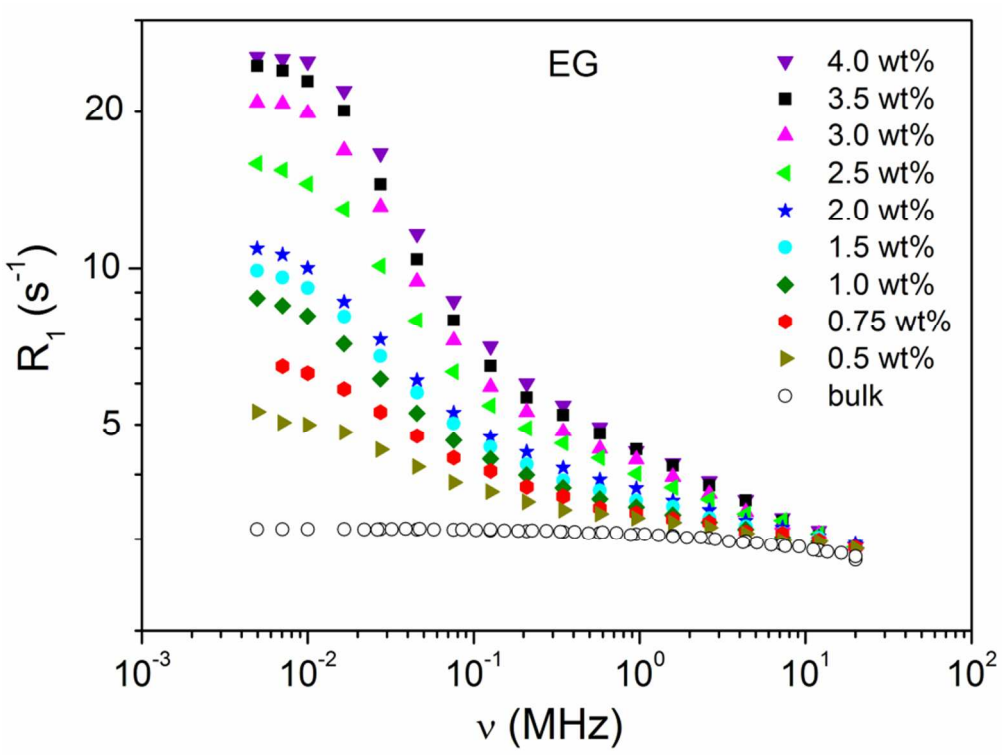

Figure 2a
82x62mm (300 x 300 DPI)

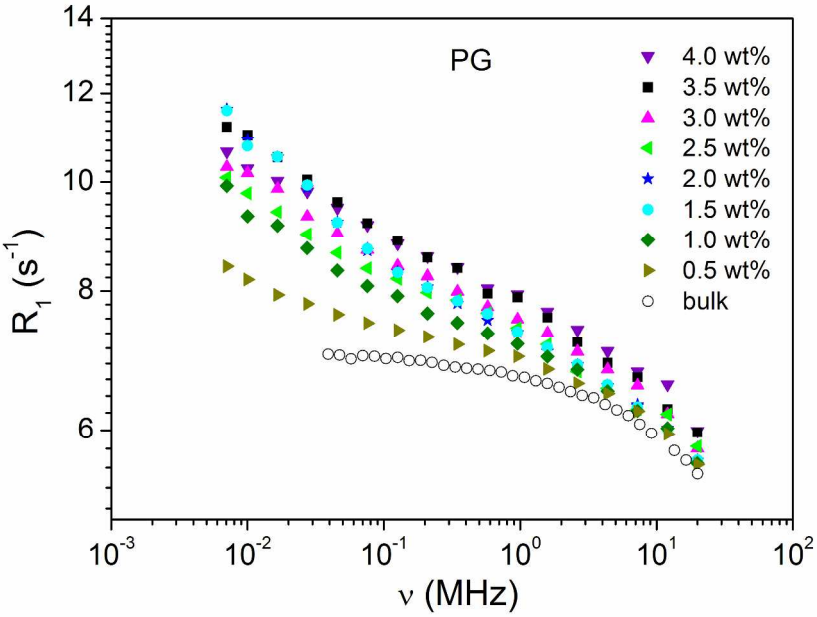

Figure 2b
288x201mm (300 x 300 DPI)

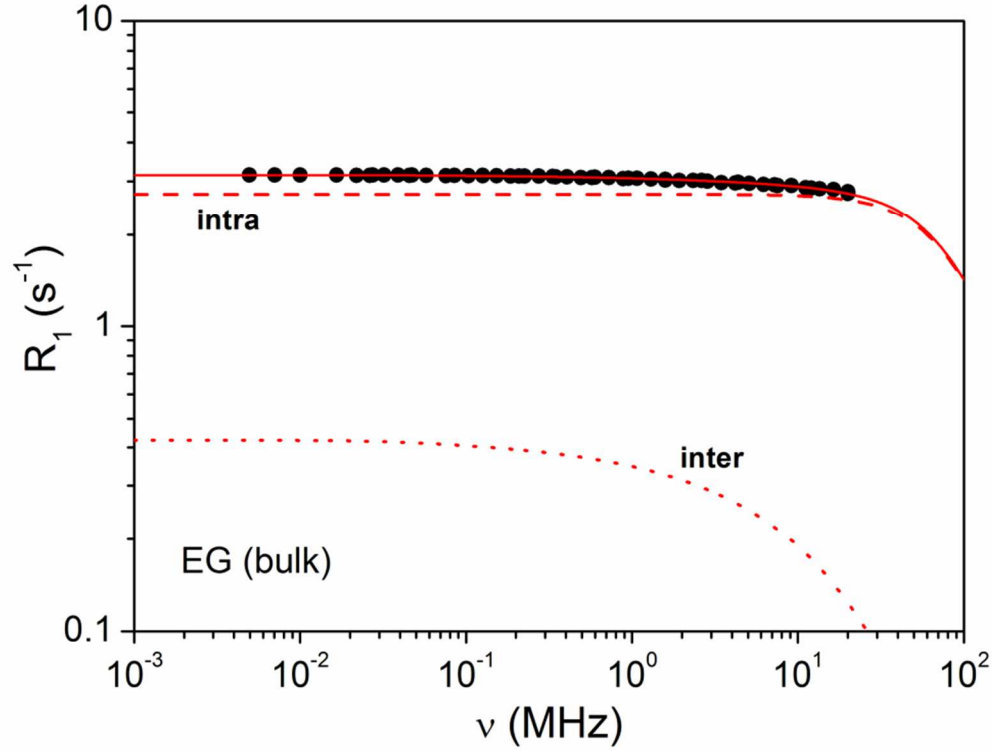

Figure 3a
82x62mm (300 x 300 DPI)

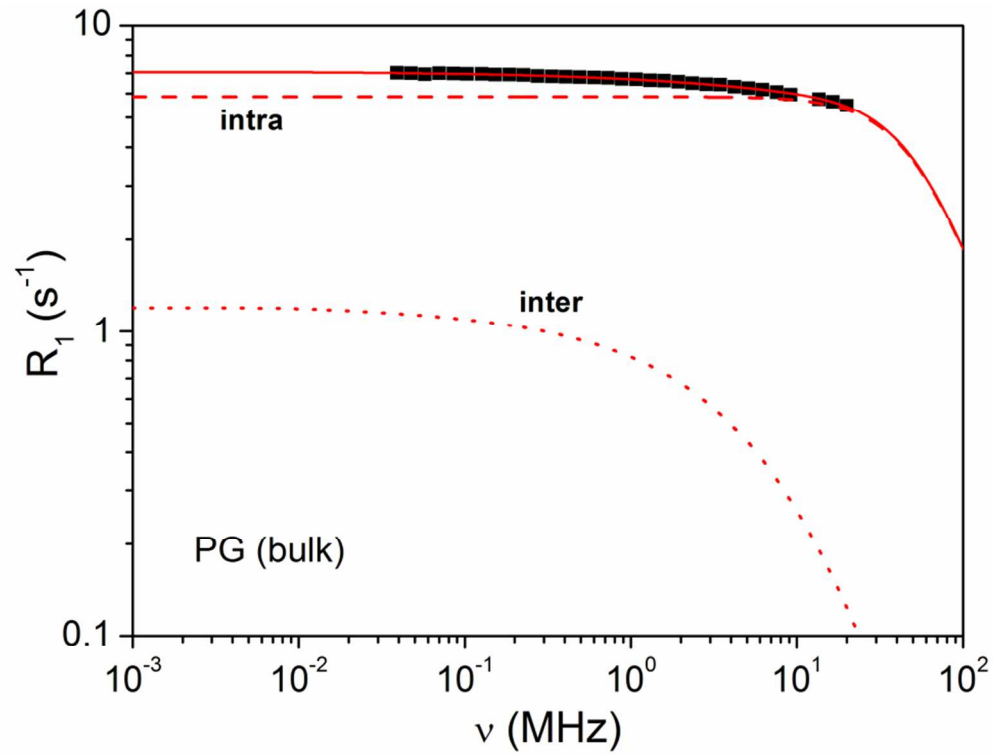

Figure 3b
82x62mm (300 x 300 DPI)

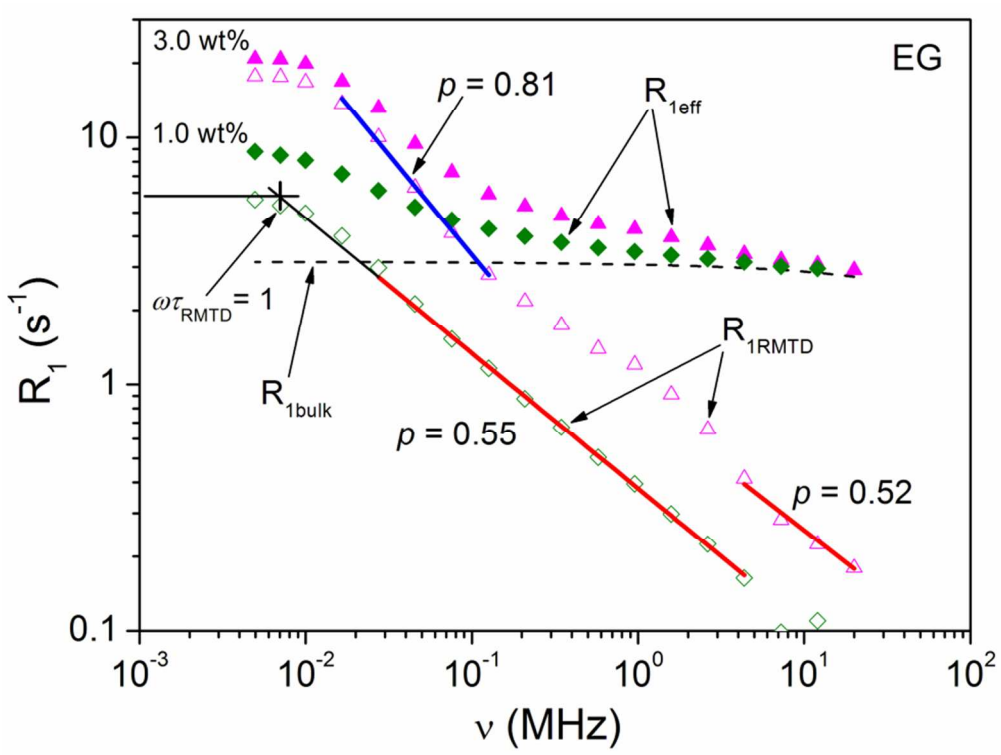

Figure 4a
82x62mm (300 x 300 DPI)

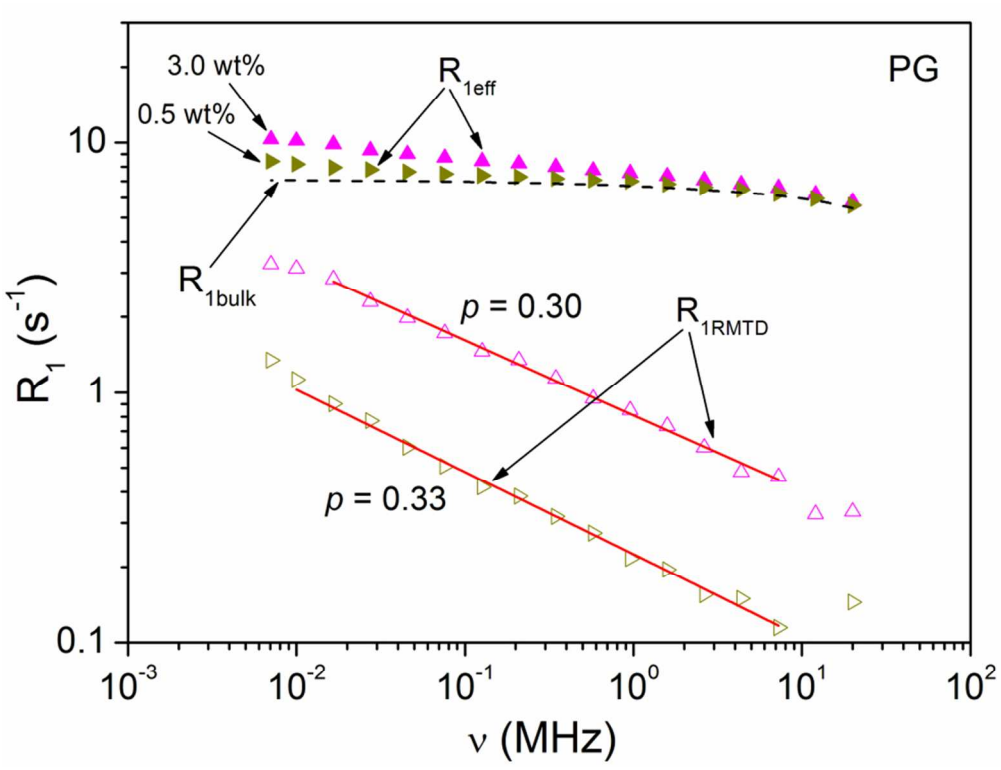

Figure 4b
82x63mm (300 x 300 DPI)

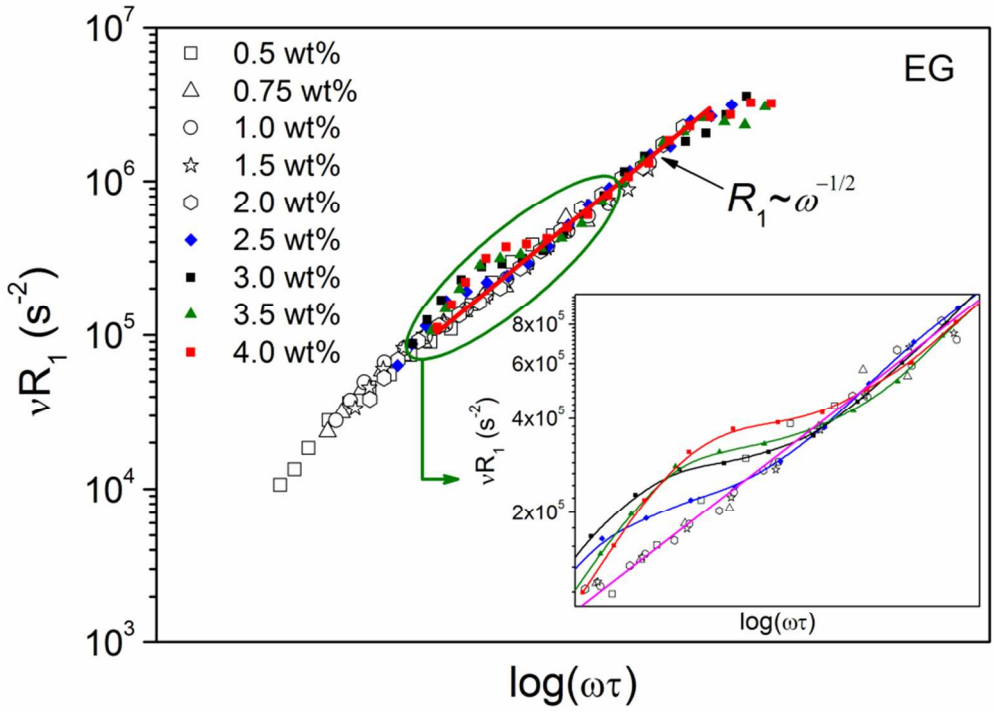

Figure 5
82x59mm (300 x 300 DPI)

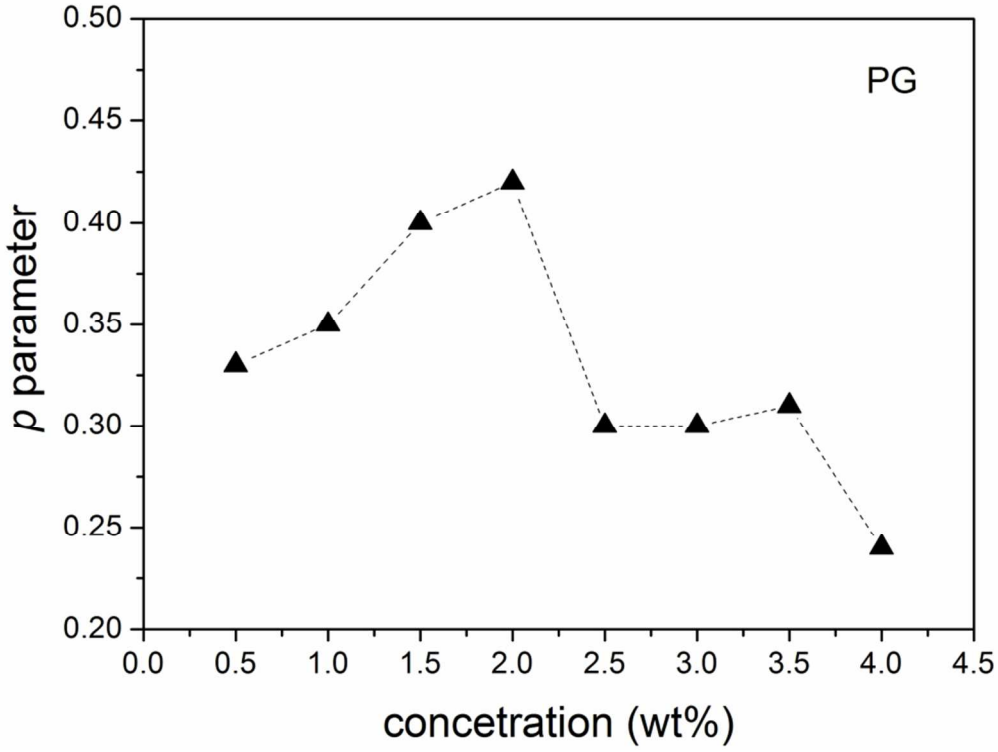

Figure 6
82x62mm (300 x 300 DPI)

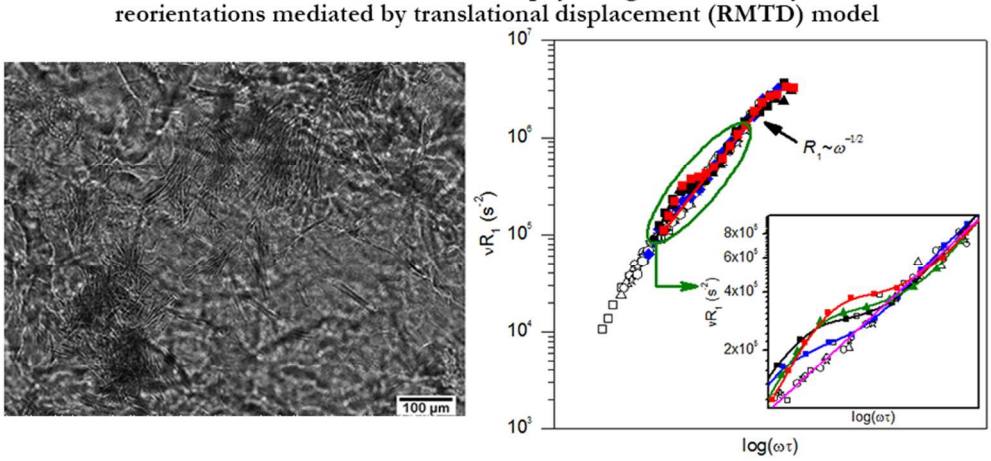

80x39mm (300 x 300 DPI)